EDGE ARTICLE

Check for updates

Effect of curvature and placement of donor and acceptor units in cycloparaphenylenes: a computational study†

Terri C. Lovell, [ID] Kaylin G. Fosnacht, Curtis E. Colwell [ID] and Ramesh Jasti [ID] *

Cycloparaphenylenes have promise as novel fluorescent materials. However, shifting their fluorescence beyond 510 nm is difficult. Herein, we computationally explore the effect of incorporating electron accepting and electron donating units on CPP photophysical properties at the CAM-B3LYP/6-311G** level. We demonstrate that incorporation of donor and acceptor units may shift the CPP fluorescence as far as 1193 nm. This computational work directs the synthesis of bright red-emitting CPPs. Furthermore, the nanohoop architecture allows for interrogation of strain effects on common conjugated polymer donor and acceptor units. Strain results in a bathochromic shift *versus* linear variants, demonstrating the value of using strain to push the limits of low band gap materials.

Introduction

Conjugated polymers are highly versatile materials used as bioimaging agents,[1–3] chemical sensors,[4–6] and components in electronic devices[7–9] including solar cells.[10] Their versatility stems from tunable optoelectronic properties. The polymer band gap is finely controlled to tune absorption and emission wavelength through incorporation of electron donating or electron accepting (electronic modulating) monomers or by increasing the quinoidal character.[11] A wide variety of known electronic modulating units are reported and significant effort is put forth to find the best donor–acceptor pairs.[12] However, one dimension of these electronic modulating units that has not been probed in conjugated polymers is the bending effect.

An ideal system to systematically test bending, and resulting strain effects, on donating and accepting monomers is the nanohoop framework, which is a cyclic arrangement of polyphenylenes (Fig. 1). The simplest nanohoop, a cycloparaphenylene (CPP), can be considered a small molecule polymer because its cyclic geometry results in quasi infinite conjugation.[13] The gap in the frontier molecular orbitals of the nanohoop narrows with increasing strain, therefore, strain may act as an additional dimension to tune conjugated polymer properties. CPPs have been used both as a monomer and additive to tune the properties of semiconducting polymers.[14,15]

However, few examples of common electronic modulating units incorporated into conjugated macrocycles exist, especially highly strained ones.[16–19] Incorporation of electron modulating units into nanohoops will allow the systematic study of strain influences as well as the impact on CPP photophysical properties.

It is challenging to make bright, stable CPPs with a small HOMO–LUMO gap due to limiting strain based reactivity and symmetry based fluorescence quenching for small CPPs.[20] However, red-emitting CPPs that retain enhanced solubility and brightness may be desirable as they show promise in applications where aggregation is problematic, such as spin coated thin film electronics or biomolecule conjugation.[21,22] By incorporating electronic modulating units into CPPs we not only test strain effects on these units, but also seek useful targets for red-emitting nanohoops. Indeed, red-emitting CPPs have been obtained with this approach, however, only three acceptor units have been tested to date.[23–25] Herein, we computationally investigate the effect of donor and acceptor moieties on CPP photophysical properties using density functional theory (DFT, TD-DFT). This work illuminates viable synthetic targets for red-

Department of Chemistry & Biochemistry, Materials Science Institute, Knight Campus for Accelerating Scientific Impact, University of Oregon, Eugene, OR 97403, USA. E-mail: rjasti@uoregon.edu

† Electronic supplementary information (ESI) available: Structures of all nanohoops analyzed, photophysical properties, NICS information, and StrainViz details (PDF) additionally, output files are provided for coordinates. See DOI: 10.1039/d0sc03923c
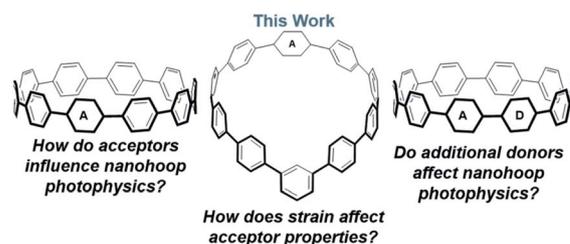

Fig. 1 Probing the effects of donor and acceptor units and strain on CPP photophysics.

emitting CPPs and demonstrates strain effects on common conjugated polymer monomers.

Computational methods

All molecules were optimized using a 6-311G** basis set and CAM-B3LYP functional with the self-consistent reaction field solvent model set to the dielectric constant of dichloromethane. All structures were confirmed to be a local energy minimum by analytical frequency analysis. Absorbance and fluorescence transitions were analyzed using GaussSum (thermal broadening of 1500 cm^{-1}). StrainViz was performed using the available software with the same functional and basis set.[26] Nuclear independent chemical shift (NICS) was calculated using aroma with 6-311+G* basis set and B3LYP functional. All calculations were performed using Gaussian-09 suite.[27]
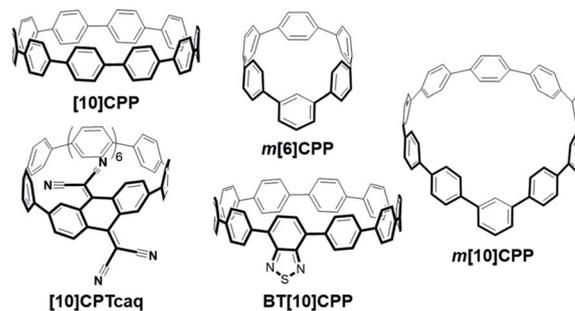
Results and discussion

The purpose of this investigation is to propose realistic targets for synthesis. We aim to propose targets with a reasonable chance of synthesis and stability. Our group and others have often run into stability issues for derivatives with high strain.[25,28–30] Therefore, we chose [10]CPP as the main scaffold for this study as it has previously shown a high tolerance to strain based reactivity.[20,23–25] The optimized ground state geometry, absorbance, optimized excited state geometry, and fluorescence of each nanohoop was calculated. The trends observed in the fluorescence were rationalized using supporting evidence from StrainViz and NICS calculations. The donor or acceptor unit replaced one phenylene to keep the conjugation and strain of the phenylene backbone relatively consistent.

Benchmarking the computational method

As the fluorescence of the nanohoops is the focus of the study, we calculated the emission of nanohoops with known experimental values shown in Fig. 2. The error in these calculations is low, between 0.2–6.3%. [10]CPTcaq is an outlier due to its solvatochromic nature. Experimentally the emission of [10]CPTcaq in carbon tetrachloride and benzene differs by over 30 nm, however, computationally there is only a 2 nm difference. This error is not a concern for this study because the solvatochromic nature also leads to reduced quantum yield. Therefore, molecules that are calculated to behave similarly are undesirable synthetic targets for bright red-emitting CPPs. By considering these relationships between calculated and experimental results, nanohoops with bright red-shifted emission can be proposed for synthesis.

Observed optoelectronic properties related to computational analysis

CPPs are unique carbon nanostructures. Due to symmetry rules, the HOMO → LUMO transition is Laporte forbidden.[31,32] Since the fluorescence is from the S$_{1'}$ → S$_0$ transition, the nanohoop HOMO–LUMO energy gap does not necessarily predict their fluorescence. The fluorescence arises from a lower lying S$_{1'}$

Fig. 2 Experimental and calculated fluorescence and associated error of [10]CPP, m[10]CPP, m[6]CPP, BT[10]CPP, and [10]CPTcaq. Error calculated in cm^{-1}.

	Experimental Emission [nm (cm^{-1})]	Calculated Emission [nm (cm^{-1})]	% Error
[10]CPP	466 (21459)	467 (21413)	0.2%
m[10]CPP	456 (21929)	463 (21598)	1.5%
m[6]CPP	510 (19607)	544 (18382)	6.3%
BT[10]CPP	571 (17513)	594 (16835)	3.9%
[10]CPTcaq	611 (16367)	506 (19763)	20.8%

state, which exhibits exciton localization and symmetry breaking resulting in a Laporte allowed transition. The ground state frontier molecular orbitals (FMOs) of larger nanohoops are delocalized over the entire phenylene backbone, whereas the S$_{1'}$ FMOs are localized over usually about seven phenylenes.[31] When the CPP FMO structure is changed, certain desirable CPP fluorescent properties, such as high quantum yield, can be lost. For example, [10]CPTcaq exhibits intramolecular charge transfer (ICT), which is responsible for decreasing the quantum yield.[25] [10]CPTcaq is a donor–acceptor molecule where the HOMO and LUMO of the S$_{1'}$ are separated. While the fluorescence is dramatically red-shifted, the quantum yield decreases by 92% to 0.05.[23] However, when CPP orbital structure is retained, the fluorescence red-shifts without losing quantum yield. BT[10]CPP and [10]CPP have similar FMO localization and fluoresce through the same mechanism, so while the emission of BT[10]CPP is red-shifted over 100 nm the quantum yield remains unchanged from [10]CPP.[25] Importantly, even though acceptors (and donors in this work) are incorporated, the resultant molecules are not donor–acceptor systems. Furthermore, the unit cannot be simply appended to the nanohoop (S4), it must be within the nanohoop and, therefore, strained. With this knowledge, accurately predicting red-shifted CPP emission with retained brightness using entirely computational methods is possible. Therefore, a wide variety of nanohoops are explored to direct synthesis of promising fluorophores.

Analysis of accepting moiety incorporation into [10]CPP and comparison to linear derivatives

Many electron accepting units are used to construct conjugated polymers.[12] We analyzed common units and explored their ability to alter CPP fluorescence. Only promising units are discussed (see ESI† for full list). A single acceptor is incorporated into the nanohoop because inclusion of multiple electron

accepting units has a minimal impact on fluorescence (S20–S24).

2,1,3-Benzothiadiazole (BTD) is a classic benzazole acceptor used in conjugated polymers and is tolerated in CPP synthesis.[25] Therefore, we explored different BTD derivatives (S1–S3, 1–4). Most were found to show small changes in fluorescence, but addition of strongly withdrawing cyano groups, 1, causes a 70 nm (1775 cm^{-1}) red-shift (bathochromic shift) to 664 nm. However, this CPP shows multiple fluorescence contributions, indicating ICT character and, therefore, a suppressed quantum yield. The most dramatic red-shift is with 2, which has two thiadiazole moieties on one phenyl ring (benzobisthiadiazole). Benzobisthiadiazole is a particularly strong accepting moiety due to the hypervalent sulfur atom and is widely employed in narrow bandgap materials.[12,33–36] This nanohoop is expected to fluoresce in the infra-red (IR) region at 1085 nm, which is red-shifted 266 nm (2993 cm^{-1}) versus a linear polyphenylene analog (Fig. 3b). The further red emission is due to increased conjugation between neighboring phenylenes from smaller torsional angles (discussed later). This indicates that the CPP structure affords a further bathochromic shift than what is achieved in linear polymer versions.

Other benzazole acceptors were also found to finely tune nanohoop fluorescence and the same trends seen in literature hold true within these CPPs.[12] Benzoselenadiazole 3 has an emission at 642 nm and the most red-shifted is benzoimidazole 4 at 695 nm. 4 is the most red-shifted because it is non-aromatic, which was confirmed by NICS calculations on the acceptors (Table S23†). Except for this result, no obvious trend correlating the aromaticity to the degree of red-shifting was observed, likely due to competing influencing factors. 3 and 4 show a 101 nm (2908 cm^{-1}) and 91 nm (2168 cm^{-1}) bathochromic shift versus linear derivatives.

Other common non-benzazole derivatives such as diketo-pyrrolopyrroles and quinoxalines were explored, but few showed significant changes. Phenazine 5 shifts the fluorescence to 654 nm, which is a bathochromic shift from most of the benzazole derivatives. Thienothiophene 6 has an emission similar to BT[10]CPP at 585 nm. However, StrainViz analysis[26] of this thienothiophene incorporated CPP 6 revealed that there is less strain than BT[10]CPP. Furthermore, the strain is localized opposite the acceptor, (discussed later in more detail) which may provide additional acceptor stabilization in smaller nanohoops. Therefore, with this acceptor the nanohoop fluorescence could be further tuned by decreasing the hoop diameter (Fig. 3c) while remaining stable. Decreasing the size to an [8]CPP derivative 8 shifts the fluorescence 33 nm (913 cm^{-1}) to 618 nm. Shrinking the size further to a [5]CPP, 11, pushes the fluorescence to 1245 nm, which is the furthest red emitting hoop discussed. However, as the size of these nanohoops decrease the oscillator strength decreases dramatically. The thienothiophene is analogous to a phenylene in terms of orbital symmetry, consequently the S$_{1'}$ → S$_0$ transition is forbidden in the smaller hoops. Therefore, decreasing the size of thienothiophene nanohoops is not a viable method to access bright red-emitting nanohoops. Furthermore, these nanohoops would be more strained than the analogous [n]CPPs so the smaller sizes would be highly unstable.

Strain considerations when incorporating electronic modulating units

Incorporation of different units into the CPP scaffold impacts strain and, therefore, stability and fluorescence. StrainViz analysis was performed on a group of [10]CPP derivatives. As is typical with CPPs, two factors dominated the strain observed:
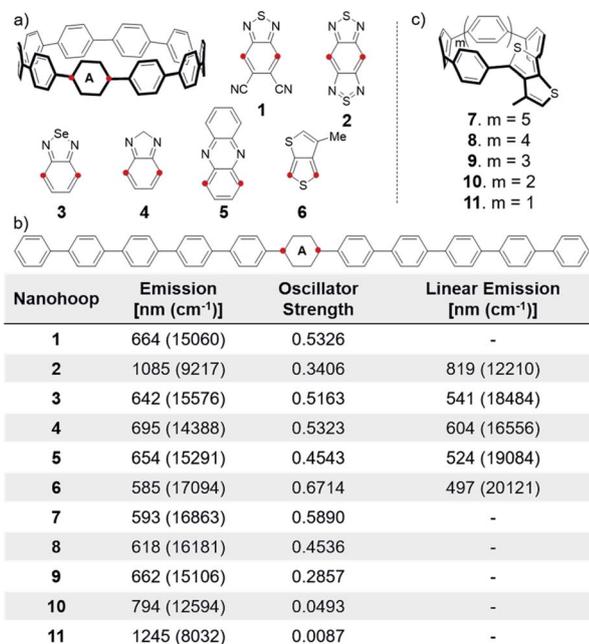

Fig. 3 Calculated emission and oscillator strength of electron accepting units in (a) [10]CPP and comparison to (b) linear derivatives as well as (c) thienothiopene acceptor in different size nanohoops. Red dots show connection points to the CPP.
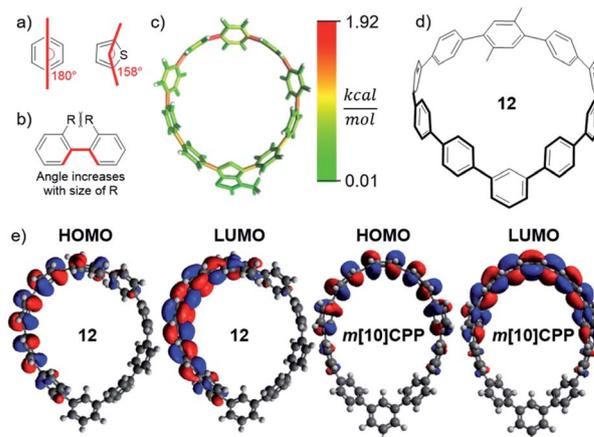
Nanohoop	Emission [nm (cm^{-1})]	Oscillator Strength	Linear Emission [nm (cm^{-1})]
1	664 (15060)	0.5326	-
2	1085 (9217)	0.3406	819 (12210)
3	642 (15576)	0.5163	541 (18484)
4	695 (14388)	0.5323	604 (16556)
5	654 (15291)	0.4543	524 (19084)
6	585 (17094)	0.6714	497 (20121)
7	593 (16863)	0.5890	-
8	618 (16181)	0.4536	-
9	662 (15106)	0.2857	-
10	794 (12594)	0.0493	-
11	1245 (8032)	0.0087	-

Fig. 4 Strain impacts in nanohoops. (a) Bending from thiophene units. (b) Impact of steric bulk on dihedral angle. (c) Thienothiophene containing nanohoop StrainViz analysis. (d) Consequences of widened dihedral angles of dimethyl-CPP 12 and (e) effect on excited state orbital distribution versus m[10]CPP.

bending (Fig. 4a) and steric bulk of the electronic modulating unit (Fig. 4b). Although they both increase strain energy, they have opposing effects on the fluorescence.

The thienothiophene containing CPP **6** well illustrates the impact of bending a linear phenylene connection (180° *versus* 158°, Fig. 4a). The angle of a thienothiophene electronic modulating unit is more acute than a *para*-phenylene (Fig. 4a) which, as seen in *m*[*n*]CPPs, shifts the strain to the opposite side of the hoop as shown in Fig. 4c. In addition to shifting the strain, the dihedral angle between the unit and adjacent phenylenes enlarges leading to worse orbital overlap across this hoop segment in the ground state, however, planarization still occurs in the excited state. Therefore, an electronic modulating unit that is more bent experiences less strain, which may lead to a slight blue shift relative to unbent electronic modulating units and enhanced stability.

Steric bulk of the electron modulating unit could widen the dihedral angle, but does not shift the strain. Instead, there is an increased quantity of strain about the single bond to the adjacent phenylene (Fig. 4b). The impact of steric bulk was analyzed through the addition of two and four methyl or ethyl groups. This type of strain leads to wider torsional angles, therefore, decreased electronic communication in between the unit and adjacent phenylenes. This is illustrated in Fig. 4e, where the excited state orbitals of **12** are only localized over a portion of the phenylene backbone. The result is a wider HOMO–LUMO gap as the dihedral strain is increased and the emission is calculated to blue-shift (**S17–S19**).

As bending and increased steric bulk have counteracting effects, the total strain energy present at a position in the molecule does not perfectly correlate to how red the emission will be. To maximize red shifting strain energy, the electronic modulating unit should not introduce a bend in the nanohoop, but instead be placed across from a bend, and have minimal torsional steric strain between it and the adjacent unit. Phenylene-like electron modulating units placed across from a *meta*-phenylene satisfy these criteria and are investigated next.

How accepting unit strain affects fluorescence

As we have seen thus far, strain is responsible for most unique optoelectronic properties observed in CPPs. When an electron accepting unit is inserted within a CPP the excited state molecular orbitals are localized on the accepting unit. Therefore, we can probe the bending effect of the electron accepting unit on emissive properties. The strain in *m*[*n*]CPPs is not evenly distributed, which provides a model system to analyze strain effects on fluorescence tuning.

In *m*[*n*]CPPs, the phenylenes closest to the *meta*-connection are the least strained and the phenylene opposite the *meta*-connection is the most strained (Fig. 5c).[26] The calculated emission of **13** is 517 nm, 77 nm (2507 cm^{-1}) lower than **BT[10]CPP**. This is consistent with *m*[*n*]CPPs, which are blue-shifted relative to their [*n*]CPP counterparts. However, **13** is significantly red-shifted (54 nm, 2256 cm^{-1}) *versus* *m*[10]CPP. As the BTD unit is moved towards the back of the hoop the fluorescence red-shifts. **14** emits at 550 nm and **15** at 588 nm. **16**
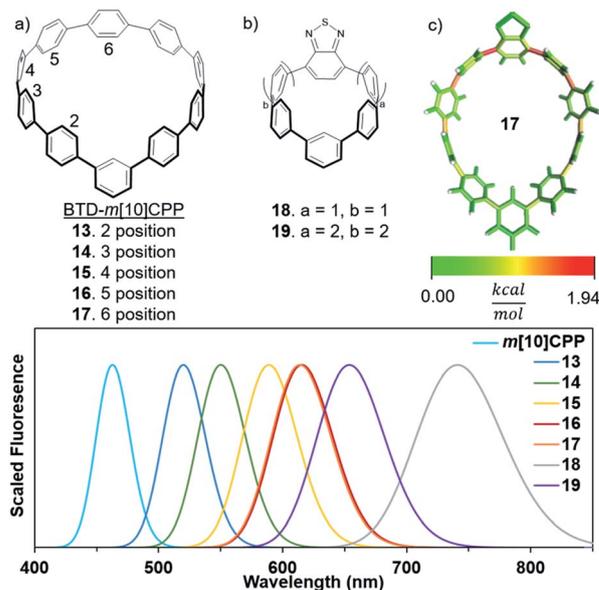

Fig. 5 Calculated emission of (a) BTD unit in different positions of *m*[10]CPP, and (b) smaller CPPs to analyze strain effects on acceptor properties. (c) Strain analysis of BTD incorporated *m*[10]CPP.
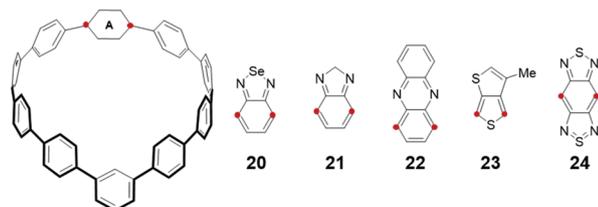
and **17** are very similar in strain and emit at 615 nm and 613 nm. Analysis using StrainViz shows an increase in acceptor strain from 2.8 to 7.0 kcal mol^{-1} depending on acceptor position. The strain can be further increased by decreasing the size of the BTD-containing *m*[*n*]CPP (**18** and **19**). Increasing strain shifts fluorescence to 799 nm for **19**. However, from a previous study these highly strained nanohoops are predicted to be unstable.[25] Therefore, to elicit a further red-shift in fluorescence without dramatically increasing the strain, other promising electron acceptors were inserted into a *m*[10]CPP scaffold.

As expected, incorporation of other acceptors into a *m*[10]CPP results in a bathochromic shift relative to their [10]CPP versions (Fig. 6). Nanohoop **20** emits 35 nm (805 cm^{-1}) further red than **3** at 677 nm. **21** shows a mere 6 nm (123 cm^{-1}) shift, which is within error of **4**. The furthest red emitting nanohoop is **24** with an emission in the infra-red (1108 nm). Although these *meta*-nanohoops have less total strain than the *para*-nanohoops, the local strain across from the *meta* phenylene is slightly higher leading to this expected red shift in emission. Advantageously, incorporation of acceptors into *meta*-nanohoops provides flexibility to balance emission tuning with stability of the molecule. If the acceptor is unstable directly across from the *meta*-linkage the acceptor can be placed in an alternative position with less strain. Furthermore, strain tuning in *m*[*n*]CPPs could allow the synthesis of smaller hoops, while avoiding acceptor instability, as an additional method to red-shift fluorescence.

Incorporation of donor and acceptor units

As mentioned above, an effective method to red-shift fluorescence is incorporation of both acceptors and donors into the molecule. Since the HOMO is localized on the acceptor in the S$_{1'}$ state, addition of donors next to the acceptors will raise the
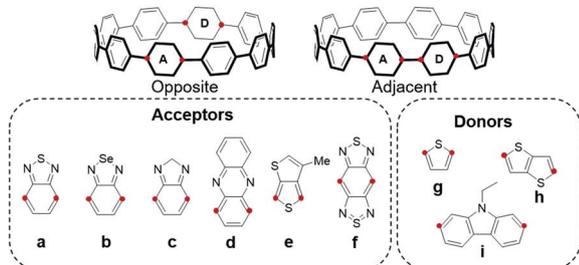
Fig. 6 Comparison of electron accepting units in *m*[10]CPP *versus* [10]CPP and as a linear polyphenylene. Red dots show connection points to the CPP.

Nanohoop	Emission [nm (cm⁻¹)]	Difference from [10]CPP version [nm (cm⁻¹)]
20	677 (14771)	35 (805)
21	701 (14265)	6 (123)
22	684 (14620)	30 (671)
23	608 (16447)	23 (647)
24	1108 (9025)	23 (192)

HOMO, decreasing the HOMO–LUMO gap in the $S_{1'}$ and red-shifting the fluorescence. We observed that the distance between the donor and acceptor moieties affects the photophysical properties. Therefore, two relative positions of the

Fig. 7 Calculated emission of [10]CPP with acceptors (a–f) and donors (g–i) in two relative positions. Comparison to linear polyphenylenes with the donors an acceptors. Red dots show connection points to the CPP.

Acceptor and donor	Adjacent Emission [nm (cm⁻¹)]	Opposite Emission [nm (cm⁻¹)]	Linear Emission [nm (cm⁻¹)]
a + g	649 (15408)	607 (16474)	584 (17123)
b + g	697 (14347)	638 (15674)	604 (16556)
c + g	747 (13387)	693 (14430)	659 (15175)
d + g	678 (14749)	632 (15823)	610 (16393)
e + g	573 (17452)	587 (17036)	533 (18762)
f + g	1161 (8613)	1084 (9225)	954 (10482)
a + h	659 (15175)	597 (16750)	581 (17212)
b + h	725 (13793)	648 (15432)	611 (16367)
c + h	762 (13123)	688 (14535)	670 (14925)
d + h	687 (14556)	649 (15408)	599 (16694)
e + h	615 (16260)	517 (19342)*	537 (18622)*
f + h	1193 (8382)	1064 (9398)	975 (10256)
a + i	578 (17301)	587 (17036)	532 (18797)
b + i	633 (15798)	606 (16502)	558 (17921)
c + i	666 (15015)	676 (14793)	621 (16103)
d + i	603 (16584)	645 (15504)	534 (18727)
e + i	560 (17857)	559 (17889)	500 (20000)
f + i	1017 (9833)	1029 (9718)	848 (11792)

*Linear derivative is further red than opposite position in nanohoop because here donor and acceptor proximity trumps strain effects.

donor and acceptor are explored and reported for all combinations of donors and acceptors, shown in Fig. 7.

The nanohoop emission with thiophene donors is further red when the donor and acceptor are adjacent to each other. As described above, there is phenylene planarization leading to orbital localization in the $S_{1'}$. When the donor and acceptor are across from each other, planarization only occurs at the acceptor and the donor is not affecting the excited state FMOs. In the case where they are adjacent, however, planarization occurs across both and the donor influences the HOMO in the ground and excited state resulting in a destabilization and consequential red-shift. However, when carbazole (**i**) is the donor the fluorescence is further red when the donor and acceptor are across from each other. This is because carbazole **i** is not a strong donor like **g** and **h**. Instead, the dominant factor is the strain increase at the opposite side of the nanohoop. When the acceptor is in this position, it results in a more red-shifted emission. This is counteracted in the case of acceptor **e** due to the strain localization being offset by the 158° thienothiophene connection (*versus* 180°).

The emissions of nanohoops with both a donor and acceptor are further red than nanohoops with just the acceptor. Additionally, nanohoops with just the donors (**S12, S15, S16**) have relatively unperturbed electronics. The furthest red-shifted emissions are seen with donor **h**. This donor is geometrically optimal with less torsional strain than a phenylene[37] and a linear connection. The acceptor responsible for the furthest red emission is **f**. A nanohoop with **f** and **h** has an emission of 1193 nm, which is 108 nm (835 cm⁻¹) further red-shifted than **2** and 85 nm than **24** (643 cm⁻¹). Incorporation of two donors on either side of the acceptor further shifts the emission (**S6**), however, incorporation of three consecutive electronic modulating units becomes challenging synthetically. Not surprisingly, nanohoops containing donor and acceptor units are further red emitting than the linear derivatives, highlighting the value of macrocyclic architecture and strain.

Directing synthesis of red-shifted nanohoops

The main purpose of this study is to direct synthetic efforts to nanohoop derivatives that are further red-shifted than ever before. With a firm understanding of acceptor unit effects in CPPs, we turn to experiment in order to make novel red-emitting nanohoop fluorophores. Since BTD incorporation is known to produce stable nanohoops (**BT[10]CPP**), exploration of this acceptor with a donor would be a rational starting point. As for other acceptors, benzobisthiadiazole is an obvious top choice since this acceptor outperformed the others by a landslide (**2** and **24**). Benzoimidazole (**4** and **21**) looks like a promising acceptor in terms of emission, however this unit is non-aromatic so it may be unstable. The benzoselenadiazole (**3** and **20**) would be the next best benzazole derivative. Lastly, we would suggest phenazine (**5** and **22**). An anthracene incorporated [12]CPP has been previously synthesized, and although this species experiences light and oxygen sensitivity, the additional nitrogen atoms in phenazine reduce the propensity for oxidative decomposition and dimerization.[38] For integrating

both a donor and acceptor in the nanohoop, thienothiophene **h** is the donor of choice since it does not dramatically alter the nanohoop structure, produces the lowest torsional angles, and has the least steric bulk. An experimental study comparing the recommended acceptors in a **[10]CPP** and *m*[**10]CPP** as well as with a thienothiophene donor would be interesting. If stable, these molecules would extend the emission of CPPs further into the red than ever before.

Conclusions

The nanohoop is a fascinating nanostructure with significant potential as a novel fluorescent material. These nanostructures are still in their infancy, and until now no systematic study of how to push their fluorescence far into the red existed. Substitution of phenyl motifs with electron accepting moieties may red-shift the fluorescence. The fluorescence of the nanohoop is further shifted through increasing the strain on the electron accepting unit through placement in a *m*[*n*]CPP. Lastly, incorporation of donors like thienothiophene **h** along with electron acceptors push the emission even further. By combining strain and appropriate electronic modulating groups such as benzo-bisthiadiazole, benzoselenadiazole, and phenazine it may be possible to shift emission to the IR. The future of highly emissive red-emitting CPPs is bright.

Conflicts of interest

There are no conflicts to declare.

Acknowledgements

Notes and references

1 T. F. Abelha, C. A. Dreiss, M. A. Green and L. A. Dailey, *J. Mater. Chem. B*, 2020, **8**, 592–606.

2 G. Hong, Y. Zou, A. L. Antaris, S. Diao, D. Wu, K. Cheng, X. Zhang, C. Chen, B. Liu, Y. He, J. Z. Wu, J. Yuan, B. Zhang, Z. Tao, C. Fukunaga and H. Dai, *Nat. Commun.*, 2014, **5**, 1–9.

3 C. G. Qian, Y. L. Chen, P. J. Feng, X. Z. Xiao, M. Dong, J. C. Yu, Q. Y. Hu, Q. D. Shen and Z. Gu, *Acta Pharmacol. Sin.*, 2017, **38**, 764–781.

4 D. T. Mcquade, A. E. Pullen and T. M. Swager, *Chem. Rev.*, 2000, **100**, 2537–2574.

5 Y.-J. Zhao, K. Miao, Z. Zhu and L.-J. Fan, *ACS Sens*, 2017, **2**, 842–847.

6 J. Tropp, M. H. Ihde, E. R. Crater, N. C. Bell, R. Bhatta, I. C. Johnson, M. Bonizzoni and J. D. Azoulay, *ACS Sens*, 2020, **5**, 1541–1547.

7 A. Facchetti, *Chem. Mater.*, 2011, **23**, 733–758.

8 X. Guo, M. Baumgarten and K. Müllen, *Prog. Polym. Sci.*, 2013, **38**, 1832–1908.

9 A. Marrocchi, A. Facchetti, D. Lanari, S. Santoro and L. Vaccaro, *Chem. Sci.*, 2016, **7**, 6298–6308.

10 G. Li, W. H. Chang and Y. Yang, *Nat. Rev. Mater.*, 2017, **2**, 1–13.

11 P. O. Morin, T. Bura and M. Leclerc, *Mater. Horizons*, 2016, **3**, 11–20.

12 M. H. Chua, Q. Zhu, T. Tang, K. W. Shah and J. Xu, *Sol. Energy Mater. Sol. Cells*, 2019, **197**, 32–75.

13 M. R. Talipov, R. Jasti and R. Rathore, *J. Am. Chem. Soc.*, 2015, **137**, 14999–15006.

14 G. M. Peters, G. Grover, R. L. Maust, C. E. Colwell, H. Bates, W. A. Edgell, R. Jasti, M. Kertesz and J. D. Tovar, *J. Am. Chem. Soc.*, 2020, **142**, 2293–2300.

15 J. Mun, J. Kang, Y. Zheng, S. Luo, H. C. Wu, N. Matsuhisa, J. Xu, G. J. N. Wang, Y. Yun, G. Xue, J. B. H. Tok and Z. Bao, *Adv. Mater.*, 2019, **31**, 1903912.

16 B. Zhang, M. T. Trinh, B. Fowler, M. Ball, Q. Xu, F. Ng, M. L. Steigerwald, X.-Y. Zhu, C. Nuckolls and Y. Zhong, *J. Am. Chem. Soc.*, 2016, **138**, 16426–16431.

17 M. Ball and C. Nuckolls, *ACS Cent. Sci.*, 2015, **1**, 416–417.

18 H. Ito, Y. Mitamura, Y. Segawa and K. Itami, *Angew. Chemie Int. Ed.*, 2015, **54**, 159–163.

19 H. Thakellapalli, B. Farajidizaji, T. W. Butcher, N. G. Akhmedov, B. V. Popp, J. L. Petersen and K. K. Wang, *Org. Lett.*, 2015, **17**, 3470–3473.

20 E. Kayahara, R. Qu and S. Yamago, *Angew. Chemie Int. Ed.*, 2017, **56**, 10428–10432.

21 E. J. Leonhardt, J. M. Van Raden, D. Miller, L. N. Zakharov, B. Alemán and R. Jasti, *Nano Lett.*, 2018, **18**, 7991–7997.

22 E. J. Leonhardt and R. Jasti, *Nat. Rev. Chem.*, 2019, **3**, 672–686.

23 T. Kuwabara, J. Orii, Y. Segawa and K. Itami, *Angew. Chem. Int. Ed.*, 2015, **54**, 9646–9649.

24 E. R. Darzi, E. S. Hirst, C. D. Weber, L. N. Zakharov, M. C. Lonergan and R. Jasti, *ACS Cent. Sci.*, 2015, **1**, 335–342.

25 T. C. Lovell, Z. R. Garrison and R. Jasti, *Angew. Chem. Int. Ed.*, 2020, **59**, 14363–14367.

26 C. E. Colwell, T. W. Price, T. Stauch and R. Jasti, *Chem. Sci.*, 2020, **11**, 3923–3930.

27 M. J. Frisch and *et al.*, *Gaussian 09*, Gaussian, Inc., Wallingford CT, Rev. E.01., 2013.

28 E. Kayahara, V. K. Patel and S. Yamago, *J. Am. Chem. Soc.*, 2014, **136**, 2284–2287.

29 P. J. Evans, E. R. Darzi and R. Jasti, *Nat. Chem.*, 2014, **6**, 404–408.

30 T. C. Lovell, C. E. Colwell, L. N. Zakharov and R. Jasti, *Chem. Sci.*, 2019, **10**, 3786–3790.

31 L. Adamska, I. Nayyar, H. Chen, A. K. Swan, N. Oldani, S. Fernandez-Alberti, M. R. Golder, R. Jasti, S. K. Doorn and S. Tretiak, *Nano Lett.*, 2014, **14**, 6539–6546.

32 Symmetry broken acene-inserted cycloparaphenylenes: R. Franklin-Margarejo, D. Ondarse Alvarez, S. Tretiak and S. Fernandez-Alberti, *Sci. Rep.*, 2016, **6**, 31253.

33 K. Ono, S. Tanaka and Y. Yamashita, *Angew. Chem. Int. Ed.*, 1994, **33**, 1977–1979.

34 H. A. M. Van Mullekom, J. A. J. M. Vekemans, E. E. Havinga and E. W. Meijer, *Mater. Sci. Eng.*, 2001, **32**, 1–40.

35 Y. Wang, T. Kadoya, L. Wang, T. Hayakawa, M. Tokita, T. Mori and T. Michinobu, *J. Mater. Chem. C*, 2015, **3**, 1196–1207.

36 F. Ye, W. Chen, Y. Pan, S. H. Liu and J. Yin, *Dye. Pigment.*, 2019, **171**, 107746.

37 D. Hashemi, X. Ma, R. Ansari, J. Kim and J. Kieffer, *Phys. Chem. Chem. Phys.*, 2019, **21**, 789–799.

38 P. Li, B. M. Wong, L. N. Zakharov and R. Jasti, *Org. Lett.*, 2016, **18**, 1574–1577.